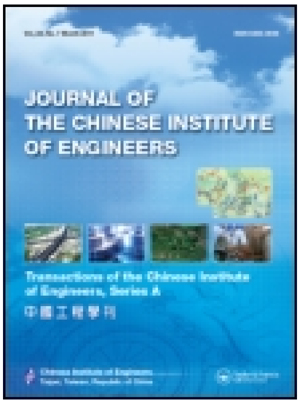

Journal of the Chinese Institute of Engineers
Publication details, including instructions for authors and subscription information:
http://www.tandfonline.com/loi/tcie20

Heat transfer of porous medium with random porosity model in a laminar channel flow

Wu-Shung Fu [a], Ke-Nan Wang [a] & Wen-Wang Ke [a]
[a] Department of Mechanical Engineering, National Chiao Tung University, Hsinchu, Taiwan 300, R.O.C.

Published online: 03 Mar 2011.

To cite this article: Wu-Shung Fu, Ke-Nan Wang & Wen-Wang Ke (2001) Heat transfer of porous medium with random porosity model in a laminar channel flow, Journal of the Chinese Institute of Engineers, 24:4, 431-438

To link to this article: http://dx.doi.org/10.1080/02533839.2001.9670640

HEAT TRANSFER OF POROUS MEDIUM WITH RANDOM POROSITY MODEL IN A LAMINAR CHANNEL FLOW

Wu-Shung Fu*, Ke-Nan Wang and Wen-Wang Ke
Department of Mechanical Engineering
National Chiao Tung University
Hsinchu, Taiwan 300, R.O.C.

Key Words: random porosity, porous medium, channel flow.

ABSTRACT

In this paper, force convection heat transfer of a porous medium in a laminar channel flow is numerically investigated. The porous medium with random porosities is used to enhance heat transfer and the random porosities are derived by the Kinderman-Ramage procedure. The results show that when the mean porosity is larger than 0.5, the average Nusselt numbers are enhanced and better than the solid block case. Therefore, a porous medium with larger porosity and the proper bead diameter could provide more heat dissipation. For the random porosity distribution, the profiles of velocities are disordered and the channeling effect is not apparent near the plate region.

I. INTRODUCTION

Recently, numerous investigations of heat and mass transport phenomena in porous media which can simulate many industrial applications such as heat exchangers, packed-sphere beds, electronic cooling, chemical catalytic reactors, drying processes, and heat pipe technology have been studied numerically and experimentally.

The porosity is one of the main parameters for studying porous media. Two major models are used to define the distribution of porosity in porous media for conveniently investigating the phenomena of thermal and flow fields. The one in which the porosity distributed in the porous medium is uniform is called the constant porosity model. Vafai and Tien (1981) used local volume averaging analysis to derive the governing equations of fluid flow and heat transfer for a porous medium.

However, Roblee *et al*. (1958) and Benenati and Brosilow (1962) observed that porosity varied significantly in the near wall region. Schwartz *et al*. (1952) conducted experimental studies and measured the maximum velocity, which is normally called the channeling effect, in the near wall region. These phenomena directly validated the idea that porosity regarded as a variable was more realistic. Then Hsu and Cheng (1990) utilized the volume averaging method to derive the governing equations for porous media. The effects of inertial term, solid boundary and variable porosity were considered. Cheng *et al*. (1991) pointed out that porosity was simulated as a damped oscillatory function of the distance from the wall and the damped oscillatory phenomenon was insignificant as the distance was larger than five bead diameters for packed beds. Therefore, concerning both practical use and a convenient theoretic model, the variation of the porosity is assumed to be an exponential function of the distance from the solid wall and is called a variable porosity model.

Besides, Georgiadis *et al*. (1987, 1988, 1991) studied unidirectional flow and heat transport phe-

*Correspondence addressee

nomena in a random porous medium. The results indicated the mean flow rate $\overline{U(\varepsilon)}$ based on random porosity was larger than that $U(\overline{\varepsilon})$ based on constant porosity when the Forchheimer model of flow was held. Saito *et al*. (1995) studied effects of the porosity and void distributions on the permeability by the Direct Simulation Monte Carlo method and found that the permeability depended, strongly, not only on the porosity but also on the void distribution. These facts indicated that except for special screen processes the sizes of the beads are extremely difficult to keep uniform.

In fact, the porosity distributions of porous media seldom agree with the distributions of the constant or variable porosity model mentioned above. That the porosity in porous media is irregular or random is more realistic. This porosity distribution is conveniently named as a random porosity model. Although the effect of random porosity distribution on the flow field has been discussed in the past, most discussions only concentrated on special phenomena. Fu and Huang (1999) studied the flow and thermal fields of a porous medium with random porosity distribution under a laminar slot impinging jet. The results showed that the porosity near the heat wall should be smaller for enhancing the heat transfer rate of an impinging jet flow.

This numerical simulation intends to adopt the random porosity model to simulate the heat transfer of a porous medium which is mounted on a horizontal hot plate in a laminar channel flow. Differet mean porosities and standard deviations are taken into consideration. The results show that the distributions of velocities U and V are chaotic and disordered in a random porosity distribution. The channelling effect is not apparently near the hot plate in the random porosity model. A porous medium with small mean porosity, $\overline{\varepsilon}$, or small bead diameter, D_p, could result in reduction of thermal performance.

II. PHYSICAL DESCRI¨ IO©

The physical model is shown in Fig. 1. A porous medium is mounted on a hot plate in a channel. The height of the channel is h. The length l_p and height h_p of the porous medium are same and equal to $h/2$. The inlet velocity distribution $u(y)$ of the fluid is fully developed and the inlet temperature T_o of the fluid is constant. The hot plate is mounted with the porous medium and the other regions are insulated. The length of the hot plate is l_p (=$h/2$), and the temperature of this region is T_w which is higher than T_o. The whole computation domain is large enough for fully developed distributions of the velocity and temperature at the outlet, ($l1$=8hp and $l2$=60hp).

In order to facilitate the analysis, the following

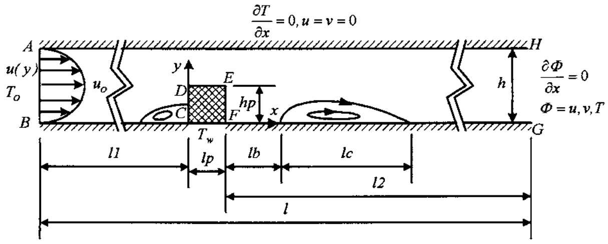

Fig. 1 Physical model

assumptions are made. (1) The material of porous medium is copper bead. (2) The flow field is steady, two-dimensional, single phase, laminar and incompressible. (3) The fluid properties are constant based on $T_{ref}=T_o+\frac{1}{3}(T_w-T_o)$ and the effect of gravity is neglected. (4) The effective viscosity of the porous medium equals to the viscosity of the external fluid.

The permeability K and inertia factor F of porous medium proposed by Vafai (1984) are defined as follows.

$$K=\frac{\varepsilon^2 dp^2}{150(1-\varepsilon)^2} \tag{1}$$

$$F=\frac{1.75}{\sqrt{150}\,\varepsilon^{1.5}} \tag{2}$$

The effective thermal conductivity k_e of a porous medium is a combination of the solid conductivity k_s and the fluid conductivity k_f validated by Shonnard and Whitaker (1989) for a high ratio of k_s/k_f.

$$k_e=k_f(4\cdot\ln(\frac{k_s}{k_f})-11) \tag{3}$$

Based on the above assumptions, the governing equations, boundary conditions and geometric dimensions are normalized in tension forms as follows:

1. Governing equations of the external flow field.

$$\frac{\partial U_i^{\langle f\rangle}}{\partial X_j}=0 \tag{4}$$

$$U_j^{\langle f\rangle}\frac{\partial U_i^{\langle f\rangle}}{\partial X_j}=-\frac{\partial P^{\langle f\rangle}}{\partial X_i}+\frac{1}{Re}\frac{\partial^2 U_i^{\langle f\rangle}}{\partial X_j^2} \tag{5}$$

$$U_j^{\langle f\rangle}\frac{\partial \theta^{\langle f\rangle}}{\partial X_j}=\frac{1}{Re\cdot Pr_f}\frac{\partial^2 \theta^{\langle f\rangle}}{\partial X_j^2} \tag{6}$$

2. Governing equations of the internal flow field proposed by Cheng (1987) for the porous medium.

$$\frac{\partial U_i^{\langle p\rangle}}{\partial X_j}=0 \tag{7}$$

$$U_j^{\langle p\rangle}\frac{\partial}{\partial X_j}\left(\frac{U_i^{\langle p\rangle}}{\varepsilon}\right)=-\frac{\partial P^{\langle p\rangle}}{\partial X_i}+\frac{1}{Re}\frac{\partial^2 U_i^{\langle p\rangle}}{\partial X_j^2}-\frac{1}{Re\,Da}\varepsilon U_i^{\langle p\rangle}$$

$$-\frac{F\left|\overrightarrow{U}^{\langle p\rangle}\right|}{\sqrt{Da}}\varepsilon U_i^{\langle p\rangle} \tag{8}$$

$$U_j^{\langle p\rangle}\frac{\partial\theta^{\langle p\rangle}}{\partial X_j}=\frac{\partial}{\partial X_j}\left(\frac{1}{Re\cdot Pr_p}\frac{\partial\theta^{\langle p\rangle}}{\partial X_j}\right) \tag{9}$$

where

$X_i=x_i+h$,

$U_i=u_i/u_o$, $P=p/\rho u_o^2$, $\theta=(T-T_o)/(T_w-T_o)$,

$Pr=\nu/\alpha$, $Da=K/H^2$, $Re=u_o h/\nu_f$,

$$\left|\overrightarrow{U}^{\langle p\rangle}\right|=\sqrt{U^2+V^2}^{\langle p\rangle}. \tag{10}$$

u_o: the maximum inlet velocity.

3. Boundary conditions

$$U^{\langle f\rangle}=0,\quad V^{\langle f\rangle}=0,\quad \frac{\partial\theta^{\langle f\rangle}}{\partial Y}=0$$

on the surfaces AH, BC, and FG. (11)

$$U^{\langle f\rangle}=-6(Y^2-Y),\quad V^{\langle f\rangle}=0,\quad \theta^{\langle f\rangle}=0$$

on the surface AB. (12)

$$\frac{\partial U^{\langle f\rangle}}{\partial X}=0,\quad \frac{\partial V^{\langle f\rangle}}{\partial X}=0,\quad \frac{\partial\theta^{\langle f\rangle}}{\partial X}=0$$

on the surface HG. (13)

$$U^{\langle p\rangle}=0,\quad V^{\langle p\rangle}=0,\quad \theta^{\langle p\rangle}=1$$

on the surface CF. (14)

The interfacial conditions at the fluid/porous medium interfaces are automatically satisfied to the Brinkman extension in the governing equations recommended by Hadim (1994).

4. Interfacial conditions on the surfaces CD and EF

$$U^{\langle f\rangle}=U^{\langle p\rangle},\quad V^{\langle f\rangle}=V^{\langle p\rangle},\quad P^{\langle f\rangle}=P^{\langle p\rangle},$$

$$\frac{\partial U^{\langle f\rangle}}{\partial X}=\frac{\partial U^{\langle p\rangle}}{\partial X},\quad \frac{\partial V^{\langle f\rangle}}{\partial X}=\frac{\partial V^{\langle p\rangle}}{\partial X},$$

$$\theta^{\langle f\rangle}=\theta^{\langle p\rangle},\quad k_f\frac{\partial\theta^{\langle f\rangle}}{\partial X}=k_e\frac{\partial\theta^{\langle p\rangle}}{\partial X}. \tag{15}$$

on the surface DE

Table 1 The main parameters

H	Hp	Lp	Dp	Re	$\overline{\varepsilon}$	σ_ε	Pr_f	Pr_p
1	0.5	0.5	0.01	500	0.5	5%	0.7	0.026
			0.1		0.7	10%		

$$U^{\langle f\rangle}=U^{\langle p\rangle},\quad V^{\langle f\rangle}=V^{\langle p\rangle},\quad P^{\langle f\rangle}=P^{\langle p\rangle},$$

$$\frac{\partial U^{\langle f\rangle}}{\partial Y}=\frac{\partial U^{\langle p\rangle}}{\partial Y},\quad \frac{\partial V^{\langle f\rangle}}{\partial Y}=\frac{\partial V^{\langle p\rangle}}{\partial Y},$$

$$\theta^{\langle f\rangle}=\theta^{\langle p\rangle},\quad k_f\frac{\partial\theta^{\langle f\rangle}}{\partial Y}=k_e\frac{\partial\theta^{\langle p\rangle}}{\partial Y}. \tag{16}$$

III. NUMERICAL SCHEME

The SIMPLEC algorithm with TDMA solver is used to solve the governing Eqs. (4)-(9) for the flow and thermal fields. Staggered and non-uniform meshes are used. The finer meshes are set in the front and rear regions of the porous medium and at the inlet and outlet regions. Non-uniform meshes with a scale ratio of 1.1 are adopted. The uniform meshes are placed in the porous medium. The harmonic mean formulation of thermophysical properties is used to avoid the effects of abrupt change of these properties across the interfacial regions of the porous medium and the external flow field for accuracy of computation. The under-relaxation factors are 0.3~ 0.5 for both the fields of velocity and temperature. The conservation residues of the equations of momentum, energy and continuity and the relative errors of each variable are used to examine the convergence criteria and defined as follows:

$$\left(\Sigma\left|Residue\ of\ \Phi\ equation\right|_{C.V.}^{2}\right)^{1/2}\le 10^{-4},$$

$\Phi=U$, V, and θ. (17)

$$\frac{\max\left|\Phi^{n+1}-\Phi^{n}\right|}{\max\left|\Phi^{n+1}\right|}\le 10^{-5},\quad \Phi=U,\ V,\ P \text{ and } \theta \tag{18}$$

In this paper, the parameters which include the Reynolds number, Re, mean porosity, $\overline{\varepsilon}$, standard deviation, σ_ε, mean diameter of beads, Dp, Prandtl number, Pr, height of the porous medium, Hp, length, Lp, inlet temperature, θ_o, and the hot plate temperature, θ_w, are tabulated in Table 1. The results of grid tests are listed in Table 2, 214×80 meshes in the domain and 40×40 meshes in the porous medium are chosen.

The distribution of porosity follows the random

Table 2 Grid tests for the case of *Re*=500, *Hp*=0.5, *Lp*=0.5, $\overline{\varepsilon}$=0.5, σ_ε=10% *Dp*=0.1 and *Pr*=0.7.

Meshes of X (A+B+C)	Meshes of Y (D+E)	$\overline{Nu}$
150 (54+16+80)	32 (16+16)	48.41
166 (60+20+86)	40 (20+20)	47.95
192 (68+30+94)	60 (30+30)	47.52
214 (74+40+100)	80 (40+40)	47.62
226 (76+46+104)	92 (46+46)	47.50
234 (78+50+106)	100 (50+50)	47.13

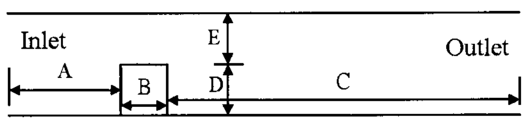

porosity model. According to Fu and Huang (1999), the theoretical form of the porosity distribution of the random porosity model is generated from the Kinderman-Ramage procedure, which is used to generate a random variable, ξ, of the standard normal distribution, $N(0,1)$, first. The random variable, ξ, is transformed to gain a general random variable, ε, corresponding to a general normal distribution, $N(\overline{\varepsilon}, \sigma_\varepsilon^2)$, of which the mean, $\overline{\varepsilon}$, and standard deviation, σ_ε, are equal to designed constants, respectively. Therefore, the distribution of the general random variable, ε, is regarded as the porosity distribution of the random porosity model in this study.

Since infinite random patterns can be generated with a given mean porosity $\overline{\varepsilon}$ and standard deviation σ_ε, it is difficult to solve all patterns. Therefore, only a few patterns with the mean porosity $\overline{\varepsilon}$ (=0.5 and 0.7) and standard deviation σ_ε (=5% and 10%) are presented to investigate the heat transfer performance of the porous medium with the random porosity model.

IV. RESULTS AND DISCUSSION

In Figs. 2(a)-(c), the global porosity distribution maps of the three selected cases of $\overline{\varepsilon}$=0.5, 0.7 and σ_ε=5%, 10% are shown. In the global porosity distribution maps, the total area of each case is approximately divided into several different porosity regions with different grey scales and the darker scale represents the smaller porosity. The maps show that the higher the standard deviation, σ_ε, is, the larger the fluctuation of the porosity distribution becomes. The higher the mean porosity, $\overline{\varepsilon}$, is, the larger local pore size is.

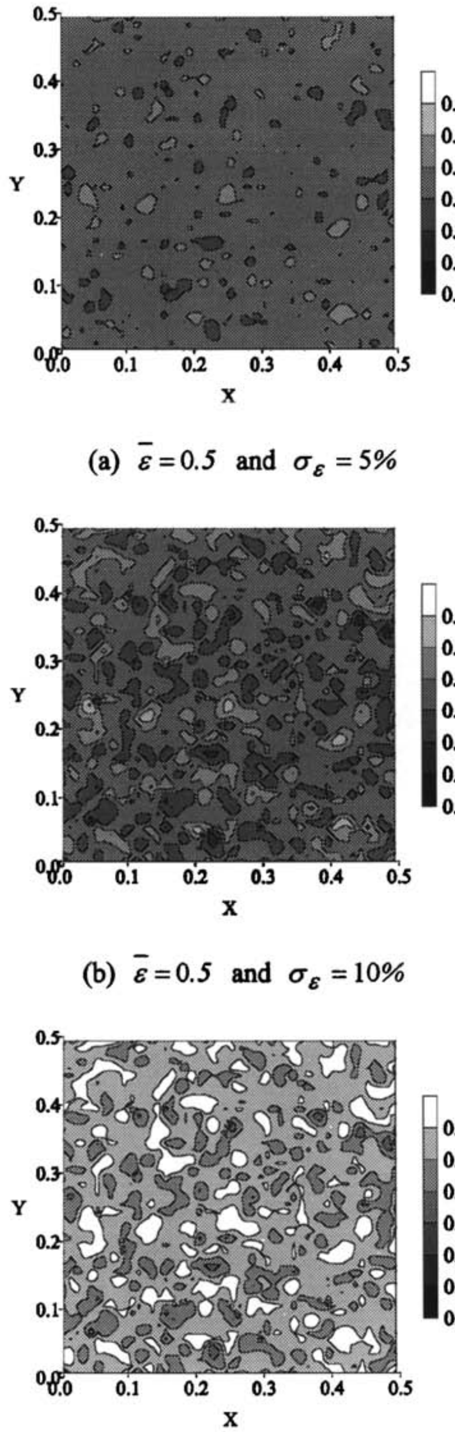

(a) $\overline{\varepsilon}=0.5$ and $\sigma_\varepsilon=5\%$

(b) $\overline{\varepsilon}=0.5$ and $\sigma_\varepsilon=10\%$

(c) $\overline{\varepsilon}=0.7$ and $\sigma_\varepsilon=10\%$

Fig. 2 Global random porosity distribution maps

To illustrate the flow and thermal fields more clearly, only the phenomena near the porous medium are presented. The region shown in the figure of the flow field is 1*h* upstream and 2.5*h* downstream from the porous medium. As shown in Fig. 3, there are streamlines for different $\overline{\varepsilon}$ and *Dp* cases. The

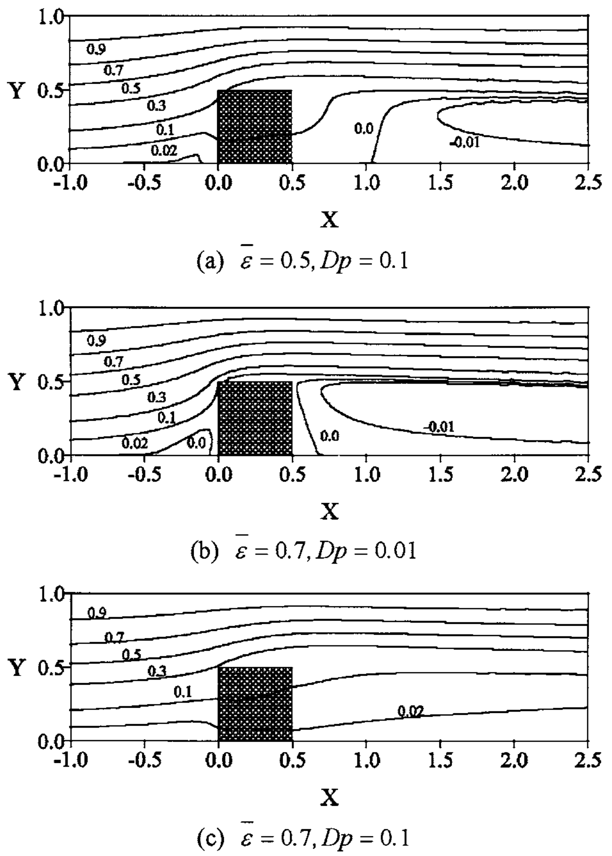

Fig. 3 Streamlines of different cases with standard deviation σ_ε=100%

dimensionless stream function, ψ, is defined as and

$$U = \frac{\partial \psi}{\partial Y} \text{ and } V = -\frac{\partial \psi}{\partial Y} \tag{19}$$

In Figs. 3(a) and (b), two recirculation zones are found in both the upstream and downstream regions from the porous medium. Since the flow penetrates into the porous medium, the downstream recirculation zone is hardly neighboring to the porous medium. In Fig. 3(b), the copper bead is smaller and the resistance becomes larger which results in the fluid hardly flowing through the porous medium. This situation is disadvantageous to the heat transfer rate of the hot plate. When Dp becomes larger ($\bar{\varepsilon}$=0.7) as shown in Fig. 3(c), the streamline of ψ=0.02 is closer to the hot plate. The results mean more fluids flow through the near wall region easily, which is advantageous to the heat transfer rate of the hot plate. The recirculation zone forms further downstream, and in the upstream region the recirculation zone is hardly observed .

As shown in Fig. 4(a), the variations of the velocity distributions of U at the middle position (X= 0.25) of the porous medium are illustrated. Due to

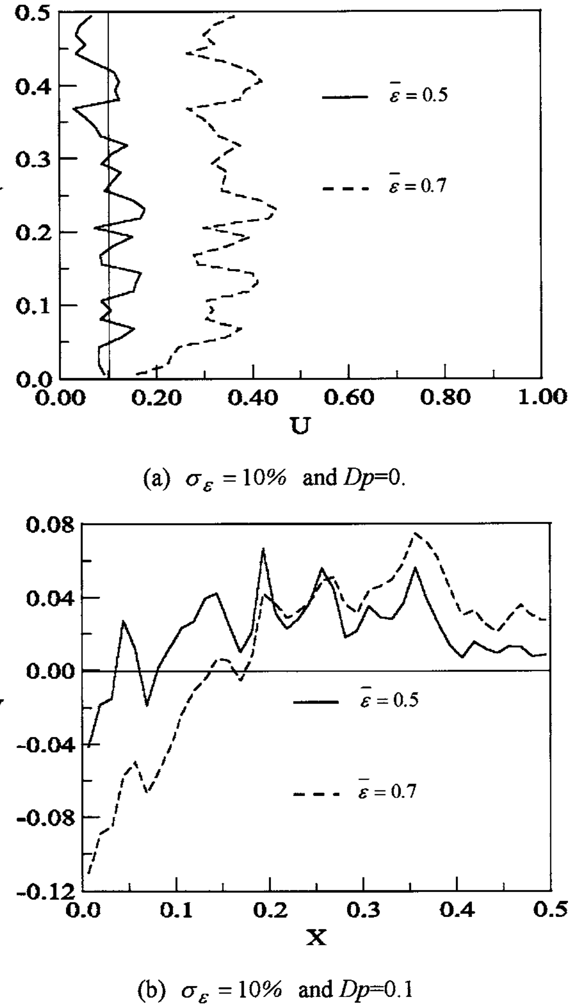

Fig. 4 (a) The profiles of velocity U of central porous medium at X=0.25. (b) The profiles of velocity V of central porous medium at Y=0.25

the drastic variations of porosity, the variations of local velocity U present jagged profiles and the channelling effect does not appear. For the different mean porosities $\bar{\varepsilon}$ (=0.5, 0.7) and the same standard deviation σ_ε (=10%) cases, the distributions of local velocity U are different. When the mean porosity, $\bar{\varepsilon}$, is larger, more fluids may flow through the porous medium, and the distribution of local velocity U becomes larger. In Fig. 4(b), the values of local velocity V are negative near the front edge of the porous medium and positive near the back edge of the porous medium. This means most fluids flow downward and flow upward through out the porous medium, which is good for the heat transfer rate at the front of the hot plate.

The isotherms accompanying Figs. 3(a)-(c) are shown in Figs. 5(a)-(c). In larger Dp cases the fluid penetrates into the porous medium, the temperature

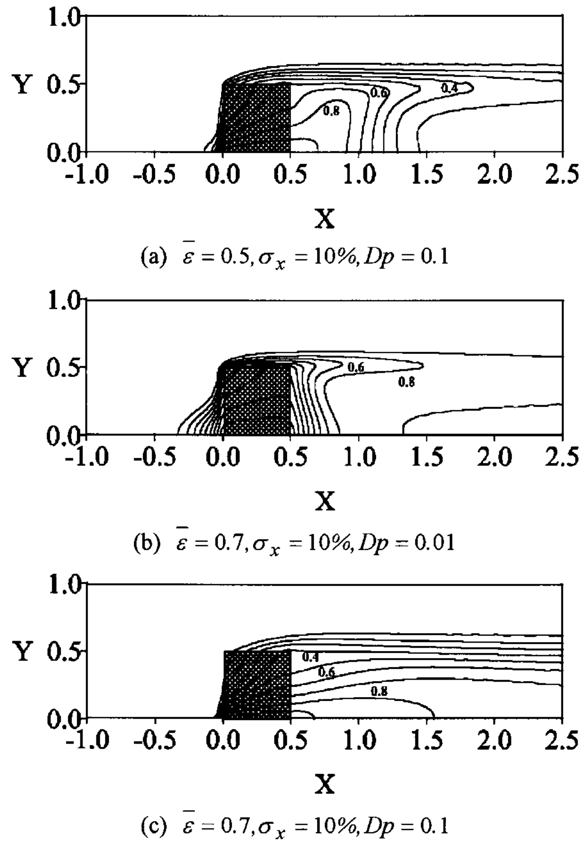

Fig. 5 Isotherms of different cases

gradient is larger and the isotherms extend farther downstream from the porous medium. On the other hand, the isotherms diffuse upstream in the (b) case with small *Dp*, and this would reduce the convective heat transfer capacity remarkably.

The local Nusselt number, *Nu*, and the average Nusselt number, $\overline{Nu}$, on the hot plate are defined as follows, respectively.

$$Nu = \frac{h_x l_x}{k_f} = -\frac{k_e}{k_f}\frac{\partial\theta}{\partial Y}\bigg|_{Y=0}, \quad h_x = \frac{q_x}{(T_w - T_0)}\bigg|_{y=0} \tag{20}$$

$$\overline{Nu} = \frac{1}{Lp}\int_0^{Lp} Nu \, dX \tag{21}$$

As shown in Fig. 6(a), based on the larger *Dp*= 0.1, due to the large contact surface between the fluids and the porous medium, the heat transfer rates are apparently enhanced for both $\bar{\varepsilon}$=0.5 and 0.7 cases compared with the cases of a solid block without porosity. The higher velocity *U* is attained for the $\bar{\varepsilon}$= 0.7 case (Fig. 4(a)). The values of *Nu* for $\bar{\varepsilon}$= 0.7 cases are then larger than those for the $\bar{\varepsilon}$=0.5 cases. For the same mean porosity, $\bar{\varepsilon}$, in Fig. 6(b), the larger *Dp* is, the larger local Nusselt number is attained. For porous medium cases, the results show that the maximum Nusselt number appears at the front of the porous medium. For a solid block case,

Table 3 The results of the different mean porosity cases based on the random porosity model under *Re*=500, σ_ε=10%, *Dp*=0.1 and *Pr*=0.7

$\bar{\varepsilon}$	$\overline{Nu}$
0.0 (Solid block)	46.85
0.4	34.44
0.5	47.62
0.6	63.62
0.7	79.70
0.8	93.58
1.0 (W. P. M.)	13.19

W.P.M. : Without porous medium

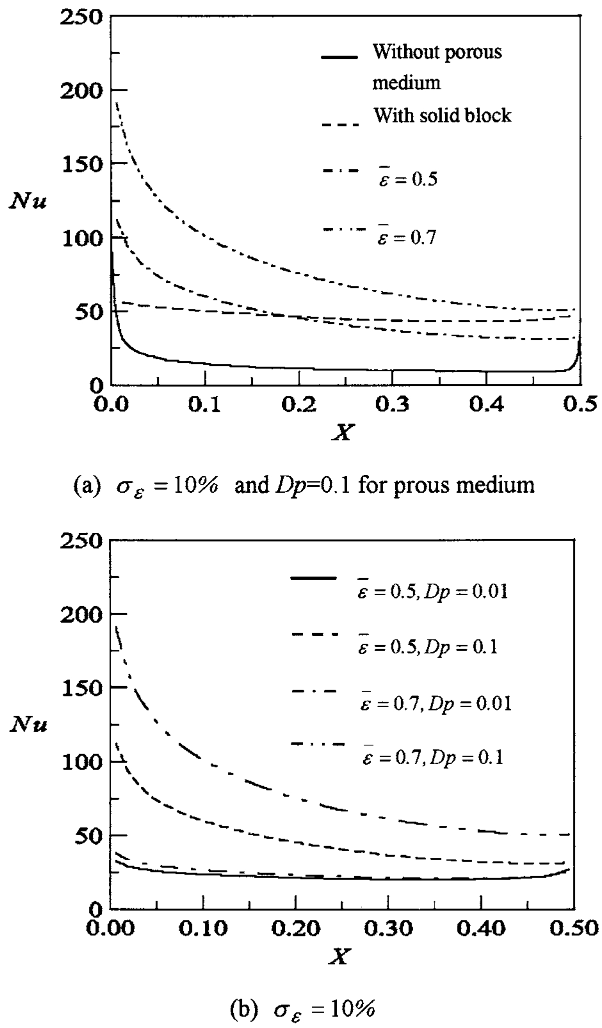

Fig. 6 The distributions of local Nusselt number *Nu* for different conditions (a) Comparison of solid block and without porous medium (b) Comparison of different bead diameters *Dp*

because of the high conductivity of copper and the existence of flow separation in the front region, the distribution of local Nusselt numbers is flatter and more uniform than those of the porous medium cases.

In Table 3, the average Nusselt number $\overline{Nu}$ of the solid block case is larger than those of $\overline{\varepsilon} \leq 0.4$ cases. The result indicates that the small mean porosity porous medium does not improve heat transfer. As the mean porosity $\overline{\varepsilon}$ is larger than 0.5, the values of $\overline{Nu}$ are larger than those of the solid block case.

V. CONCLUSIONS

The force convection heat transfer rates of a random-pore porous medium mounted on a hot plate in a laminar channel flow is numerically investigated. The main results can be summarized as follows:

1. For the random porosity model, the distributions of velocities U and V are chaotic and disordered. The channeling effect is not apparent near the plate region.
2. A porous medium with a larger porosity can provide more heat dissipation than a solid block.
3. A porous medium with small mean porosity, $\overline{\varepsilon}$, or small bead diameter, Dp, could result in reduction of thermal performance.

NOMENCLATURE

Dp	Dimensionless mean bead diameter, $Dp=dp/h$
dp	Mean bead diameter (m)
F	Inertial factor
h	Height of the channel
Hp	Dimensionless height of the porous medium, $Hp=hp/h$
h_x	Local heat transfer coefficient ($Wm^{-2}K^{-1}$)
K	Permeability (m^2)
k	Thermal conductivity ($Wm^{-1}K^{-1}$)
L	Dimensionless length
$N(a,b^2)$	Normal distribution with mean a and standard deviation b
Nu	Nusselt number
Pr	Prandtl number, $Pr=\nu/\alpha$
p	Pressure (Nm^{-2})
q_x	Local heat flux (Wm^{-2})
Re	Reynolds number, $Re=\rho u_o h/\mu$
T	Temperature (K)
U, V	Dimensionless velocity in the X- and Y-direction, respectively
u_o	Maximum inlet velocity ($msec^{-1}$)
X, Y	Dimensionless Cartesian coordinates

Greek Symbols

α	Thermal diffusivity (m^2sec^{-1})
$\overline{\varepsilon}$	Mean porosity
ξ	Random variable
ν	Kinematic viscosity (m^2sec^{-1})
θ	Dimensionless temperature
ρ	Fluid density (kgm^{-3})
σ_ε	Standard deviation of porosity
Φ	Computational variable
ψ	Dimensionless stream function

Superscripts

n	The nth iteration index
$-$	Mean value
$\rightarrow$	Velocity vector

Subscripts

e	Effective value
f	External flow field
i	Index; inlet
p	Porous medium
s	Solid block
w	Hot wall

ACKNOWLEDGMENT

The support of this work by National Science Council, Taiwan, R.O.C. under contract NSC87-2212-E-009-035 is gratefully acknowledgment.

REFERENCES

1. Benenati, R. F., and Brosilow, C. B., 1962, "Void Fraction Distribution in Packed Beds," *American Institute of Chemical Engineers Journal*, Vol. 8, pp. 359-361.
2. Catton, I., Georgiads, J. G., and Adnani, P., 1988, "The Impact of Nonlinear Convective Processes on Transport Phenomena in Porous Media," *Proceedings of 1988 National Heat Transfer Conference*, Vol. 1, ASME HTD-96, Houston, pp. 767-777.
3. Cheng, P., Chowdhury, A., and Hsu, C. T., 1991, "Forced Convection in Packed Tubes and Channels with Variable Porosity and Thermal Dispersion Effects," *In Convective Heat Mass Transfer in Porous Media*, ed. S. Kakac *et al.*, pp. 625-653.
4. Fu, W. S., and Huang, H. C., 1999, "Effects of a Random Porosity Model on Heat Transfer Performance of Porous Media," *International Journal of Heat and Mass Transfer*, Vol. 42, pp. 13-25.
5. Georgiads, J. G., and Catton, I., 1987, "Stochastic Modeling of Unidirectional Fluid Transport in Uniform and Random Packed Beds," *The*

Physics of Fluids, Vol. 30, pp. 1017-1022.

6. Hadim, A., 1994, "Forced Convection in a Porous Channel with Localized Heat Sources," *Journal of Heat Transfer*, Vol. 116, pp. 465-472.
7. Hsu, C. T., and Cheng, P., 1990, "Thermal Dissipation in a Porous Medium," *International Journal of Heat and Mass Transfer*, Vol. 33, pp. 1587-1597.
8. Georgiads, J. G., 1991, "Effect of Randomness on Heat and Mass Transfer in Porous Media," *In Convective Heat Mass Transfer in Porous Media*, ed. S. Kakac *et al*., pp. 499-524.
9. Roblee, L. H. S., Baird, R. M., and Tiern, J. W., 1958, "Radial Porosity Variations in Packed Beds," *American Institute of Chemical Engineers Journal*, Vol. 4, pp. 460-464.
10. Saito, A., Okawa, S., Suzuki, T., and Maeda, H., 1995, "Calculation of Permeability of Porous Media Using Direct Simulation Monte Carlo Method (Effect of Porosity and Void Distribution on Permeability)," *Proceedings of ASME/JSME Thermal Engineering Joint Conference*, Vol. 3, Maui, pp. 297-304.
11. Schwartz, C. E., and Smith, J. M., 1952, "Flow Distribution in Packed Beds," *Industrial and Engineering Chemistry*, Vol. 45, pp. 1209-1218.
12. Shonnard, D. R., and Whitaker, S., 1989, "The Effective Thermal Conductivity for Point Contact Porous Medium: An Experimental Study," *International Journal of Heat and Mass Transfer*, Vol. 23, pp. 503-512.
13. Vafai, K., 1984, "Convective Flow and Heat Transfer in Variable-Porosity Media," *Journal of Fluid Mechanics*, Vol. 147, pp. 233-259.
14. Vafai, K., and Tien, C. L., 1981, "Boundary and Inertia Effects on Flow and Heat Transfer in Porous Medium," *International Journal of Heat and Mass Transfer*, Vol. 24, pp. 195-203.

Manuscript Received: Jul, 17, 2000
Revision Received: Nov. 24, 2000
and Accepted: Dec. 04, 2000

槽道流中具隨機孔隙率之多孔性介質之熱傳分析

傅武雄　王可男　柯文旺

國立交通大學機械工程學系

摘　要

本文以數值計算方法探討在二維槽道中強制熱對流對隨機孔隙率多孔性介質熱傳效果之影響。本文應用具有隨機孔隙分布之多孔性介質以增強熱傳效率且孔隙率分佈是依據 Kinderman-Ramage 程序所產生。本文計算結果顯示當平均孔隙率大於0.5時，平均紐塞數有明顯增益且較固體凸塊者爲佳。因此，在較高的平均孔隙率時，配合採用適當的銅粒半徑，隨機孔隙率之多孔性介質能有較佳的散熱效果。在採用隨機孔隙率分布下，多孔性介質內部的速度呈不規則分布，近壁面處槽道效應並不明顯。

關鍵詞：隨機多孔性，多孔性材料，渠道流。